Modeling the Phase Behavior of Polymer−Clay Composites

Yulia Lyatskaya and Anna C. Balazs*

Department of Chemical and Petroleum Engineering, University of Pittsburgh, Pittsburgh, Pennsylvania 15261

Received April 29, 1998; Revised Manuscript Received July 2, 1998

ABSTRACT: To model the phase behavior of polymer−clay composites, we develop a free energy expression for a mixture of polymers and solid, thin disks. The free energy expression is adopted from the Onsager model for the equilibrium behavior of rigid rods. Thus, our theory takes into account the possible nematic ordering of the disks within the polymer matrix. By minimizing this free energy and calculating the chemical potentials, we construct phase diagrams for the polymer−disk mixtures. The findings provide guidelines for tailoring the polymer molecular weight and the volume fraction of the different components to fabricate thermodynamically stable mixtures with the desired morphology.

Introduction

Polymer−clay nanocomposites constitute a new class of materials where nanoscale clay particles are molecularly dispersed within a polymer matrix.[1−9] Such composites exhibit dramatic increases in tensile strength, heat resistance, and decreases in gas permeability when compared to the pure polymer matrix.[3] The improved properties are achieved at very low loadings of the inorganic component, namely, 1−10 wt %.[3] Thus, the new materials are lighter in weight than conventionally filled polymers.[9] These unique properties make the nanocomposites ideal materials for products ranging from high-barrier packaging for food and electronics to strong, heat-resistant automotive components.

Despite the experimental strides in synthesizing these nanocomposites,[1−9] the factors that control the formation of such hybrids are not well-understood. For example, it is not clear under what conditions the different components will become intermixed to yield thermodynamically stable materials. Yet, the desirable properties listed above will depend on the thermodynamic stability of the mixture and the overall morphology of the material. In this paper, we present a theoretical model for the equilibrium phase behavior of polymer−clay mixtures. Actual clay particles are roughly oblong in shape and possess a very high aspect ratio, being approximately 200 nm in diameter and 1 nm in width. We model these particles as thin, rigid disks and calculate phase diagrams for the polymer−disk mixture. We also discuss the possible morphology of the mixtures. The findings provide guidelines for tailoring the polymer molecular weight and the volume fraction of the different components to fabricate thermodynamically stable mixtures with the desired structure.

The Model

To investigate the behavior of polymer−clay mixtures, we model the individual clay sheets as rigid disks of diameter D and thickness L. The polymers are modeled as flexible chains of length N. The diameter of a monomer, a, is chosen as our unit of length. The composition of the mixture is characterized by the volume fraction of disks in the blend, ϕ_d. Since we assume the mixture to be incompressible, the volume fraction of polymer is given by $\phi_p = 1 - \phi_d$. The interaction between a monomeric unit in the polymer chain and a surface site on the disk is characterized by the Flory−Huggins interaction parameter, χ.

There are two critical issues that need to be addressed in a consideration of such polymer−clay, or polymer−disk, mixtures. First, it is important to isolate factors that affect the miscibility of these two components. Second, it is of particular interest to determine the morphology of the final composite. We begin by discussing the first issue and then present a simple kinetic argument, which we couple with our equilibrium analysis, to help address the second topic.

Since the disks have a high aspect ratio, we must consider that, in the mixed state, the disks can be either randomly oriented with respect to each other and form an isotropic phase or be relatively aligned and form a nematic phase. To analyze the miscibility of the polymer−disk mixture and investigate the formation of the isotropic and nematic structures, we adopt the framework of the Onsager model,[10] which was used to probe the nematic ordering of rigid rods. This formalism has several advantages over other approaches that have been used to describe liquid crystal-like ordering. In comparison to Flory-type theories,[11−13] the Onsager model[10] does not depend on a lattice for a description of the system. As compared to the Ginzburg−Landau-type theories (see, for example, ref 14), this approach is valid over a wider concentration range of rigid particles.

The starting point in this Onsager-based approach is the expression for the free energy of the mixture, which has the following form:

$$F = F_{conf} + F_{ster} + F_{int} + F_{transl} \qquad (1)$$

The term F_{conf} describes the conformational losses due to the alignment of the disks, F_{ster} accounts for the steric interactions between the disks, F_{int} describes the influence of nonspecific attractive forces between the disks, and F_{transl} takes into account the translational entropy of disks. In particular, each term is given by the following equations:

$$F_{conf} = n_d \int \mathbf{f}(\mathbf{u}) \ln(4\pi \mathbf{f}(\mathbf{u}))\, d\Omega_u \equiv \sigma \qquad (2)$$

S0024-9297(98)00687-1 CCC: $15.00
Published on Web 09/03/1998

$$F_{ster} = n_d J(\phi_d) \int\int f(\mathbf{u}_1)\, f(\mathbf{u}_2)\, B(\gamma)\, d\Omega_1\, d\Omega_2 \quad (3)$$

$$F_{int} = -\phi_d (n_d/v_d)(\Theta/T) \quad (4)$$

$$F_{transl} = n_d \ln \phi_d \quad (5)$$

Here, n_d is the number of disks in a unit volume, $v_d = (\pi D^2 L)/4$ is the volume of an individual disk, and $f(\mathbf{u})$ is the orientational distribution function. The parameter Θ denotes the Θ temperature for the system, and T is temperature. All energetic characteristics are expressed in the units of kT, where k is the Boltzmann constant.

We note that, in ref 15, F_{int} was calculated in terms of the Θ temperature, the point where the second virial coefficient is equal to zero. Recall that for polymer−rod (disk) mixtures,[10,19] the Θ temperature depends not only on enthalpic contributions but also on terms that describe the entropic losses for polymers of length N. As given below, eq 9 demonstrates the relationship among Θ, χ, and N. We further note that we do not include the anisotropic part of the attractive interactions in eq 4 since these interactions were shown[15] to play a negligible role in the phase behavior of the system.

We adopt the general form of these terms from the Onsager model, but we make a correction to account for the presence of disks, rather than rods. The $B(\gamma)$ term in eq 3 represents the second virial coefficient and is given by $B(\gamma) = b(4/\pi)|\sin \gamma|$, where b is half of the excluded volume between two rigid particles if they are randomly oriented and γ is the angle between these two particles. This term is different for disks and rods. For disks, $b = (\pi^2 D^3)/16$, whereas for rods, $b = \pi l^2 d/4$, where l is the length and d is the diameter of the rods. We also modify the term for the steric interactions between the particles. For this modification, we turn to refs 15−17, where the correction function $J(\phi_d) = -(1/v_d)\ln(1 - \phi_d)$ was introduced to extend the model beyond the limit of low concentrations of rods or, in our case, disks. The low concentration limit is the regime described by the Onsager model. As noted in ref 15, with this correction, the steric interactions are now described in a manner that is similar to the prescription in the Flory model.[11] Therefore, the two approaches should yield similar results.

To determine the region of miscibility for the polymer−disk mixture, one has to minimize the above expression for the free energy, F. This, however, will lead to an integral equation,[18] which can only be solved numerically. Instead, Onsager used the variational method with a trial function for $f(\mathbf{u})$. Here, we follow the same scheme and represent $f(\mathbf{u})$ in the following form:[19]

$$f(\mathbf{u}) = (\alpha/4\pi) \exp(-\alpha\theta^2/2) \quad (6)$$

where α is a variational parameter and θ is an angle between the director and the test disk.

Through the use of eq 6, the expression for the free energy now has the following form:

$$F = n_d\,(\text{constant} + \ln \phi_d + \sigma - \ln(1 - \phi_d)(b/v_d)\rho - \phi_d(b/v_d)(\Theta/T)) \quad (7)$$

where σ is defined in eq 2 and $\rho = (4/\pi)\langle|\sin \gamma|\rangle$. These parameters allow us to distinguish between the isotropic and nematic phases. In the isotropic phase, $\sigma = 0$, $\rho = 1$, while in the nematic phase, $\sigma_n = 2\ln(-(2/\pi^{1/2})(b/v_d)\ln(1 - \phi_d)) - 1$, $\rho_n = -2(v_d/b)/\ln(1 - \phi_d)$.

We can express Θ/T in terms of the Flory−Huggins interaction parameter, χ, by equating the expression for free energy, eq 7, in the isotropic case ($\sigma = 0$, $\rho = 1$) to the free energy expression of an isotropic mixture:[20]

$$F = n_d \ln \phi_d + n_p \ln \phi_p + \chi n_d v_d \phi_p \quad (8)$$

where n_p is the number of polymer molecules in a unit volume. Here, we consider the case where the isotropic phase is stable for low concentrations of disks and expand the logarithmic terms in eqs 7 and 8. Hence

$$\Theta/T = 1 + (\chi - {}^1/_2 N)(v_d{}^2/b) \quad (9)$$

and

$$F = n_d(\text{constant} + \ln \phi_d + \sigma - \ln(1 - \phi_d)(b/v_d)\rho - \phi_d(b/v_d) - \chi v_d \phi_d + v_d \phi_d/2N) \quad (10)$$

In the more general case, for arbitrary values of ϕ_d, the expression for the free energy has the form

$$F = n_d(\text{constant} + \ln \phi_d + \sigma - \ln(1 - \phi_d)(b/v_d) \times (\rho - 1) + \chi v_d \phi_p) + n_p \ln \phi_p \quad (11)$$

This expression for the free energy is also consistent with the free energy equation in ref 13b, where the researchers considered the behavior of a polymer−rod mixture.

To construct the equilibrium phase diagram, one has to equate the chemical potentials of the disks and polymer in the isotropic and nematic phases: $\mu^i_d = \mu^n_d$, $\mu^i_p = \mu^n_p$, where $\mu^i_k = (\delta F_i)/(\delta n_k)|_{n_{j\neq k}=\text{constant}}$. The corresponding chemical potentials are

$$\mu_p = -N/v_d(\phi_d + (\phi_d{}^2/(1 - \phi_d))(b/v_d)\rho - \phi_d{}^2(b/v_d)\Theta/T) \quad (12)$$

$$\mu_d = \text{constant} + \ln \phi_d + \sigma + (b/v_d)\rho(\phi_d - \ln(1 - \phi_d)) - \phi_d - 2\phi_d(b/v_d)\Theta/T + \phi_d{}^2(b/v_d)\Theta/T \quad (13)$$

where Θ/T is given in eq 9. We solve this system of equations numerically and present the results as plots that highlight the role of χ, ϕ_d, and N in the phase behavior of the system.

Results and Discussion

We begin our analysis by examining how the general features of the phase diagram are changed as the geometry of the solid component is altered from rod to disk. Thus, we contrast the phase behavior for rods and disks, where the respective solids are mixed with a monomeric solvent, or $N = 1$. The diameter of the disks is equal to the length of the rods, $D = l = 20$, and L, the width of the disk, is set equal to 1. Recall that all lengths are expressed in units of a, the diameter of a monomer. Figure 1 shows the phase diagrams for the different systems in the Θ/T vs ϕ coordinate frame. As noted above, the parameter Θ is the Θ-temperature for the system and T is temperature. Here, ϕ is the volume fraction of the rigid particles (rods or disks). The solid curves mark the phase boundaries for the system of rods, and the dashed curves mark these boundaries for the disks. The area between the respective boundaries encompasses the phase-separated region. The two

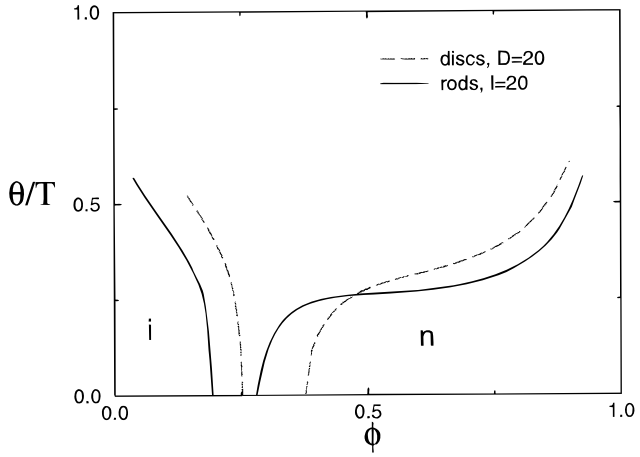

Figure 1. Phase diagrams for the rod (solid lines) and disk (dashed line) systems. The solids are mixed with a monomeric solvent. The results are plotted as a function of Θ/T vs ϕ, where ϕ is the volume fraction of the solid component. The diameter of the disks is equal to the length of the rods, $D = l = 20$, and L, the width of the disks, $= 1$. The area between the phase boundaries encompasses the region of immiscibility. The miscible regions lie below the boundaries. Within the regions of miscibility, i marks the isotropic phase and n indicates the nematic phase.

regions below the boundaries pinpoint the regions of miscibility: the mixture forms an isotropic phase (i) at low concentrations, ϕ, of rods (or disks) and exhibits an anisotropic phase, with a nematic (n) ordering of the rods (or disks) at high ϕ.

Relative to the rods, the immiscible region for the system of disks is shifted to the right, in the direction of higher ϕ values (see Figure 1). Consequently, the isotropic phase is broader and the nematic phase is narrower for the disks than the rods. In other words, the disks sustain isotropic ordering and initiate nematic ordering at higher concentrations than rods. For the rest, the phase diagrams for rods and disks appear qualitatively similar. Therefore, one can expect similar trends in the nematic ordering of disks and rods. For example, longer (more asymmetric) rods form a nematic phase at lower concentrations, i.e., the isotropic−nematic transition is shifted to lower ϕ at higher rod lengths.[17,21] Hence, the nematic ordering of disks will also be promoted by an increase in the diameter (asymmetry) of the disks. This behavior is shown in Figure 2. Note that, in the two limiting cases of low and high D, there is the possibility of isotropic−isotropic (i−i) phase coexistence in the former case and nematic−nematic (n−n) phase coexistence in the latter case. These transitions are calculated in much the same manner as that outlined above for the isotropic−nematic transitions, but we now equate the chemical potentials of two isotropic (or nematic) phases at different values of ϕ.

We now turn to the equilibrium properties of polymer−disk mixtures and focus on the effect of varying N, the degree of polymerization of the chains. Figure 3 shows the respective phase diagrams when polymers of different chain lengths are mixed with the disks. Here, the diameter of the disks is fixed at $D = 30$ and the width L is set at 1. As can be seen from the figure, the region of immiscibility increases with an increase in N. The plots further reveal that, for relatively high N ($N > 100$), phase separation occurs even at negative values of χ, where there is an attractive interaction between the two components. In other words, at $N > 100$, the polymer and disks are totally immiscible even if there is no repulsion between these components, indicating an entropically driven phase separation.

In this equilibrium analysis, the disks are assumed to be well-separated from each other. Thus, each particle could undergo random mixing with the polymer. In reality, however, this situation might not be reached. Consider the scenario where the polymer is mixed with a clay agglomerate;[6] within the agglomerate, the individual crystallites or sheets are arranged in closely spaced parallel stacks. In order for the different components to intermix, the polymer must penetrate the gap (or "gallery") between these sheets. As we discuss below, the kinetics of this process could affect the morphology and, consequently, the properties of the mixture.

Our main argument is based on the assumption that the diameter of the disks is large, and initially the disks are stacked together, like the clay sheets within the agglomerate. In this case, the polymer has to penetrate the gap between two disks from the outer edge and then diffuse toward the center of the gallery. When the polymer moves through the gap, two scenarios are possible, depending on the value of χ. In the first case, $\chi \geq 0$ and there is no attraction between the polymer and disks. Here, the polymer can separate the disks, as the chain tries to retain its coillike conformation and gain entropy. In the second case, $\chi < 0$ and the polymer and disks experience an attractive interaction. Here, the polymer "slides" through the gallery, maximizing

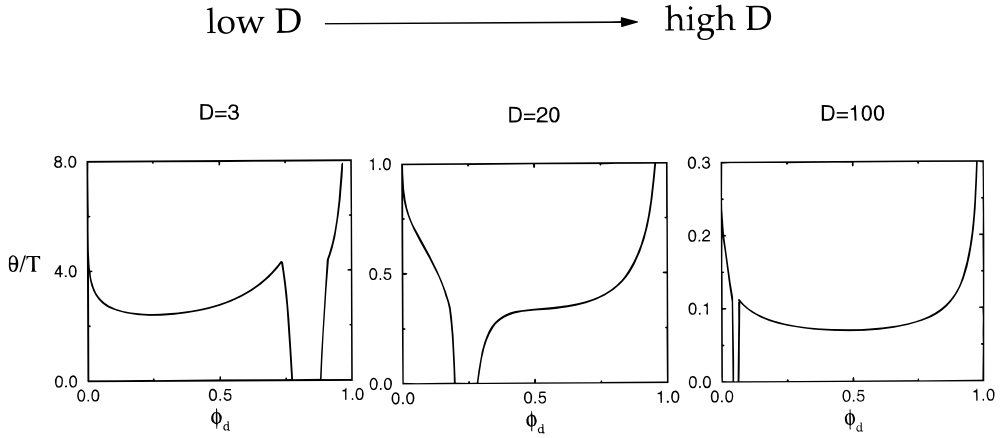

Figure 2. Plots showing the effect of increasing the diameter of the disks on the phase behavior of the system. In all the diagrams, $L = 1$. In this figure, ϕ_d represents the volume fraction of disks.

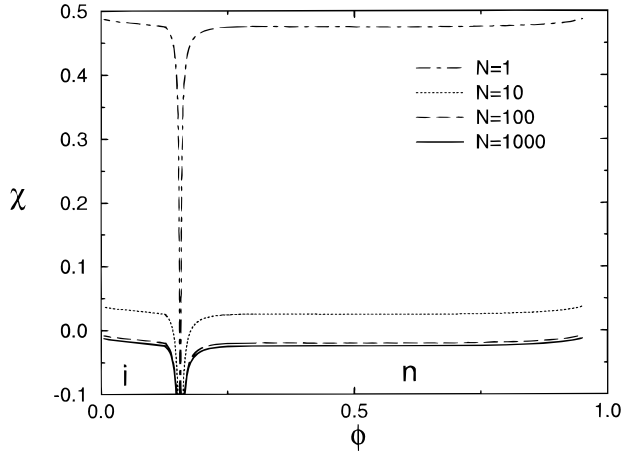

Figure 3. Phase diagrams for disks and polymers of different degrees of polymerization, N. The results are plotted as a function of χ vs ϕ, where ϕ is the volume fraction of the disks. The diameter of the disks is $D = 30$, and the width of the disks is $L = 1$. The area above the phase boundaries encompasses the region of immiscibility. The miscible regions lie below the boundaries. Within the regions of miscibility, i marks the isotropic phase and n indicates the nematic phase. The plots reveal that increasing N increases the region of immiscibility.

contact with the two confining surfaces. The overall conformation of the polymer is rather "flat", but the losses in conformational entropy are compensated by enthalpic gains when the chain comes in contact with one of the disks. (The latter behavior is similar to the surface adsorption of attractive homopolymers. Above a critical adsorption energy, the chains stick to the surface and form "trains" that lie along the substrate.[22])

The final structure of the mixture will obviously be different for the two scenarios. In the first case, the disks will be totally separated and randomly oriented in the polymer matrix. This is referred to as an exfoliated structure. In the second case, the disks are effectively glued together by the intervening polymer and the platelets remain parallel to each other. This morphology is referred to as an intercalated structure.

We can now combine the results of the equilibrium study with our kinetic arguments to analyze the structure of the final composite. As discussed in the paragraph above, a true exfoliated structure, where the disks are totally separated, can only occur for $\chi \geq 0$. The equilibrium analysis, however, shows that for $\chi \geq 0$, the polymers and disks will ultimately demix *unless* the polymer is relatively short, namely, $N < 100$. Therefore, a stable exfoliated structure can only be attained by mixing disks with relatively short polymers.

Again from kinetic considerations, we observed that an intercalated structure is expected when $\chi < 0$. The equilibrium analysis (see Figure 3) shows that χ must be negative for mixtures of long polymers and disks to be thermodynamically stable. Combining these arguments, we see that stable mixtures of high molecular weight polymers and discotic particles will exhibit an intercalated morphology.

More systematic experimental studies are needed to test our prediction on the role of χ and N in determining the morphology of the mixture. Nonetheless, recent experiments on mixtures of clays and high molecular weight styrene-derivative polymers[23] show qualitative agreement with our results. Here, the derivatized polymers are polar in nature and readily interact with polar moeities on the surface of the clay; in other words, the interaction between the clays and polymer is relatively attractive.[24] The molecular weights of the chains were at least $M_w = 30\,000$ ($\approx N > 300$). As anticipated from our discussion above, all the samples exhibited an intercalated structure. Furthermore, when nonpolar polymers, which are not attracted to the surface of the clays, were employed in the process, the mixture was immiscible.

Conclusions

We present an Onsager-type theory to analyze the phase behavior of polymers and rigid disks, taking into account the possible nematic ordering of the disks. We show that the favorable mixing of the polymer and disks is controlled through a balance of the effects of N and χ. In particular, an increase in N requires a decrease in χ for the mixture to be thermodynamically stable. On the basis of simple kinetics arguments, we predict that a truly exfoliated structure is only possible for low N and $\chi > 0$. When N is high and $\chi < 0$, the mixture is expected to exhibit an intercalated morphology. In other cases, the mixture is immiscible and the material phase separates. These predictions provide useful design criteria and facilitate the cost-effective fabrication of polymer−clay composites.

In studies currently underway, we are examining the overall phase behavior of polymer/disc/solvent mixtures[25] and polymer/polymer/disc blends.[26] The findings will indicate whether the addition of small molecule solvents,[25] or other polymeric components,[26] can enhance the miscibility of the mixtures.

Acknowledgment. A.C.B. greatly acknowledges the Army Office of Research and DOE for financial support through Grant DE-FG02-90ER45438.

References and Notes

(1) Okada, A.; Kawasumi, M.; Kojima, Y.; Kurauchi, T.; Kamigaito, O. *Mater. Res. Soc. Symp. Proc.* **1990**, *171*, 45.
(2) Yano, K.; Uzuki, A.; Okada, A.; Kurauchi, T.; Kamigaito, O. *J. Polym. Sci., Part A: Polym. Chem.* **1993**, *31*, 2493.
(3) Kojima, Y.; Usuki, A.; Kawasumi, M.; Okada, A.; Kurauchi, T.; Kamigaito, O. *J. Polym. Sci., Part A: Polym. Chem.* **1993**, *31*, 983.
(4) Uzuki, A.; Kawasumi, M.; Kojima, Y.; Okada, A.; Kurauchi, T.; Kamigaito, O. *J. Mater. Res.* **1993**, *8*, 1174.
(5) (a) Uzuki, A.; Kawasumi, M.; Kojima, Y.; Okada, A.; Kurauchi, T.; Kamigaito, O. *J. Mater. Res.* **1993**, *8*, 1174. (b) Kojima, Y.; Uzuki, A.; Kawasumi, M.; Okada, A.; Fukushima, Y.; Kurauchi, T.; Kamigaito, O. *J. Mater. Res.* **1993**, *8*, 1185. (c) Giannelis, E. *Adv. Mater.* **1996**, *8*, 29.
(6) Vaia, R. A.; Jandt, K. D.; Kramer, E. J.; Giannelis, E. P. *Macromolecules* **1995,** *28*, 8080.
(7) Vaia, R. A.; Sauer, B. B.; Tse, O. K.; Giannelis, E. P. *J. Polym. Sci., Part B: Polym. Phys.* **1997**, *35*, 59.
(8) Messersmith, P. B.; Stupp, S. I. *J. Mater. Res.* **1992**, *7*, 2599.
(9) Krishnamoorti, R.; Vaia, R. A.; Giannelis, E. P. *Chem. Mater.* **1996**, *8*, 1728.
(10) Onsager, L. *Ann. N. Y. Acad. Sci.* **1949**, *51*, 627.
(11) Flory, P. J.; Abe, A. *Macromolecules* **1978**, *11*, 1119.
(12) Abe, A.; Ballauff, M. In *Liquid Crystallinity in Polymers*; Ciferri, A., Ed.; VCH Publishers: Cambridge, U.K., 1991; p 131.
(13) (a) Li, W.; Freed, K. *J. Chem. Phys.* **1995**, 103, 5693. (b) Matsuyama, A.; Kato, T. *J. Chem. Phys.* **1996**, *105*, 1654.
(14) Liu, A. J.; Fredrickson, G. H. *Macromolecules* **1993**, *26*, 2817.
(15) Khokhlov, A. R.; Semenov, A. N. *J. Stat. Phys.* **1985**, *38*, 161.
(16) Khokhlov, A. R.; Semenov, A. N. *Macromolecules* **1986**, *19*, 373.
(17) Khokhlov, A. R. In *Liquid Crystallinity in Polymers*; Ciferri, A., Ed.; VCH Publishers: Cambridge, U.K., 1991; p 97.
(18) Lekkerkerker, H. N. W.; Coulon, Ph.; Van Der Haegen, R.; Deblieck, R. *J. Chem. Phys.* **1984**, *80*, 3427.
(19) Odijk, T. *Macromolecules* **1986**, *19*, 2313.

(20) Flory, P. *Principles of Polymer Chemistry*; Cornell University Press: Ithaca, NY, 1953.
(21) Grosberg, A. Yu.; Khokhlov, A. R. *Statistical Physics of Macromolecules*, AIP Press: New York, 1994.
(22) Fleer, G.; Cohen-Stuart, M. A.; Scheutjens, J. M. H. M.;Cosgrove, T. Vincent, B. *Polymers at Interfaces*; Chapman and Hall: London, 1993; Chapter 5.
(23) Vaia, R. A.; Giannelis, E. P. *Macromolecules* **1997,** *30*, 8000.
(24) While we do not consider electrostatic interactions in this model, the strong attraction between the polar units is comparable to having a large, negative χ between the components.
(25) Lyatskaya, Y.; Balazs, A. C. Manuscript in preparation.
(26) Balazs, A. C.; Singh, C.; Zhulina, E.; Modeling the Interactions between Polymers and Clay Surfaces through Self-Consistent Field Theory. Submitted for publication in *Macromolecules*.

MA980687W